# NASA TECHNICAL MEMORANDUM

N73- 25867

NASA TM X- 62,270

NASA TM X- 62,270

CASE FILE COPY

# ALFVÉN WAVE REFRACTION BY INTERPLANETARY INHOMOGENEITIES

William D. Daily

Ames Research Center
Moffett Field, Calif. 94035

May 1973

# Alfvén Wave Refraction by Interplanetary Inhomogeneities

## WILLIAM D. DAILY[1]

Ames Research Center, NASA, Moffett Field, Calif. 94035

*Abstract.* Pioneer 6 magnetic data reveals that the propagation direction of Alfvén waves in the interplanetary medium is strongly oriented along the ambient field. Magnetic fluctuations of frequencies up to 1/30 sec in the spacecraft frame are shown to satisfy a necessary condition for Alfvén waves and a variance matrix analysis is used to determine the Alfvén wave normal. It appears from this analysis that geometrical hydromagnetics may satisfactorily describe deviation of the wave normal from the background field. The rotational discontinuity is likely also to propagate along the field lines.

## INTRODUCTION

There is now considerable evidence that plasma waves constitute much of the microscale structure of the interplanetary medium. Attention has been focused on both the theoretical and observational study of such waves, because of their importance in dynamical processes within the wind itself as well as their effects on geophysical phenomena. Theoretical work indicates that interplanetary conditions external to the corona are favorable for propagation of the Alfvén mode but most of the time the magnetosonic modes are strongly damped [*Barnes*, 1966]. The analysis of fluctuations in interplanetary magnetic and fluid parameters reveals that Alfvén waves may be present in the solar wind. No evidence has been presented that any but the Alfvén mode is abundant [*Belcher and Davis*, 1971]. This has resulted in many studies of Alfvén wave characteristics in the interplanetary plasma. In this paper we report some properties of large amplitude, aperiodic Alfvén fluctuations in the interplanetary magnetic field and relate this information to the ambient

---

[1] National Research Council postdoctoral resident research associate.

plasma properties. We will be specifically concerned with the effects of plasma inhomogeneities on the direction of wave propagation.

Some of the first evidence for the existence of Alfvén-like behavior in the solar wind plasma was offered by *Coleman* [1966, 1967] and was based on spectral studies of interplanetary parameters. About the same time *Burlaga* [1968] found several examples of wave-like structure in the Pioneer 6 data and *Unti and Neugebauer* [1968] found specific regions of plasma and magnetic data with fluctuations that appeared much like Alfvén waves.

Of particular importance to the work reported in this paper are the results of *Belcher et al.* [1969]. They found correlations greater than 0.8 between the radial components of magnetic field and proton velocity for 30% of 5 months in the Mariner 5 data. They attributed these correlations to large-amplitude aperiodic Alfvén waves propagating out from the sun. This study was later extended [*Belcher and Davis*, 1971] by showing similar correlations between vector fluctuations in the magnetic and velocity fields with the conclusion that 'Large-amplitude, nonsinisodial, Alfvén waves propagating out from the sun with a broad wavelength range from $10^3$ to $5 \times 10^6$ km dominate the microscale structure at least 50% of the time.' The best examples of these waves were found in high velocity streams and on their trailing edges, while the leading edges generally contained larger amplitude fluctuations but lower magnetic-velocity correlations. On the other hand, in low velocity streams the microscale regime was found to be a mixture of small-amplitude Alfvén waves and nonAlfvénic structure (possibly static in the plasma frame). They also reported a variance matrix analysis (described below), which showed that over a frequency range of 3 hr to 168.75 sec the direction of minimum variance in the magnetic field tends to be aligned with the mean magnetic field direction. This observation will be examined in detail below.

Closely related to microscale waves are MHD discontinuities. Some of these will be included in the analysis of this paper. Discounting hydromagnetic shocks, there are basically three types of discontinuity: 1) Contact; 2) Tangential; 3) Rotational. The contact discontinuity is not expected in the solar wind near 1 AU on theoretical grounds [*Barnes*, 1971] and has not been observed [*Burlaga*,

1971]. The tangential discontinuity has been observed by *Turner and Siscoe* [1971] and *Burlaga* [1971]. *Burlaga* [1969] found that directional discontinuities (which include tangential and rotational) have a normal defined by $\vec{B}_1 \times \vec{B}_2$, which tends to be perpendicular to the spiral direction but out of the ecliptic plane. *Turner and Siscoe* [1971] attempted to distinguish between the two types of directional discontinuities. They concluded that $\vec{B}_1 \times \vec{B}_2$ for tangential discontinuities was very nearly in the ecliptic plane along the orthospiral direction while the rotational discontinuities were approximately normal to the spiral, but had large southward components. This gives no information about the direction of the wave normal for the propagating discontinuity—$\vec{B}_1 \times \vec{B}_2$ defines a plane of 'polarization' [as defined by *Turner and Siscoe*, 1971], although a large-amplitude Alfvén wave need not be polarized in the conventional sense. The relation of this plane to the wave normal will be discussed in the next section.

## GEOMETRICAL MAGNETOHYDRODYNAMICS

The dispersion equation resulting from the hydrodynamic equations for a completely ionized, nonrelativistic magnetoplasma has three solutions. One of these allows for a nondissipative, nondispersive wave (or discontinuity) of arbitrary amplitude propagating in any direction relative to the ambient magnetic field $\vec{B}$ such that $|B|$ and the plasma density remain constant and the magnetic fluctuations are transverse to the direction of propagation [*Kantrowitz and Petschek*, 1966]. The relevant geometry is shown in Figure 1 for a wave vector inclined $\alpha$ to the mean field. The field constraints mean that $\vec{B}$ can move in any manner around the wave vector $\vec{k}$ ($k = 2\pi/\lambda$) as long as $B_{||} = \vec{B} \cdot \vec{k}/k$ and $|B|$ remain constant. The movement of $\Delta \vec{B}_{\perp}(\Delta \vec{B}_{\perp} \cdot \vec{k} = 0)$ thereby defines a plane which is normal to the propagation vector. In the small amplitude limit this plane becomes undefined. A rotational discontinuity is just a sharply crested Alfvén wave and is often characterized by another plane defined by $\vec{B}_{initial} \times \vec{B}_{final}$ that can have any orientation to $\vec{k}$. In contrast is the tangential discontinuity. Here the magnetic vector moves arbitrarily in a plane but its magnitude can vary [see *Colburn and Sonett*, 1966]. It should be emphasized here that using only magnetic field data to identify structure as Alfvénic may result in errors. For example, a tangential discontinuity with $|B|$ constant will look like an Alfvén wave

propagating normal to the mean field. A screening procedure described later will be used on the variance of the magnetic field in an attempt to identify fluctuations as Alfvén waves using only magnetic data.

Ray trajectories in an inhomogeneous plasma may be predicted by the eikonal (WKB) method. First used in geometrical optics, a generalization of this technique was shown by *Weinberg* [1962] to be useful in describing small amplitude magnetoplasma waves. The eikonal equation is derived for $L \gg k^{-1}$ where L is the length characterizing the plasma inhomogeneity. (In the data analysis to follow, the smallest scale gradients in the plasma and magnetic field will have characteristic lengths approximately 3-30 times the wave length (for further explanation see the section entitled Determination of the Wave Normal Direction.) If the dispersion equation admits wave packet solutions of circular frequency centered at $\omega(\vec{k}, \vec{x})$, the trajectory equations can be written

$$\frac{d\vec{x}}{dt} = \frac{\partial \omega}{\partial \vec{k}}$$

$$\frac{d\vec{k}}{dt} = -\frac{\partial \omega}{\partial \vec{x}}$$

These are Hamilton's equations for wave quanta of momentum $\hbar\vec{k}$ ($\hbar = h/2\pi$) and Hamiltonian $\hbar\omega$ and from them it can be shown that the wave frequency (energy) is constant along a ray. For a hydromagnetic wave the second equation is

$$\frac{d\vec{k}}{dt} = -\frac{\partial(kU)}{\partial \vec{x}} \tag{1}$$

5

where U is the local phase speed. Let us characterize the slow hydromagnetic (Alfvén) mode by

$$\omega(\vec{k},\vec{x}) = kU(\hat{k},\vec{x})$$

$$U(\hat{k},\vec{x}) = \hat{k}\cdot\vec{V}(x) + \hat{k}\cdot\hat{b}(x)C_A(\vec{x})$$

where

$$\hat{k} = \vec{k}/k$$
$$\hat{b} = \vec{B}/B$$

$\vec{V}(x)$ is the plasma bulk velocity and $C_A = B/\sqrt{4\pi\rho}$ is the Alfvén speed which is dependent on $\vec{x}$ through $\vec{B}(x)$ and $\rho(\vec{x})$. Now equation (1) is

$$\frac{\partial\omega}{\partial\vec{x}} = \vec{k}\cdot\hat{b}(\vec{x})\,\frac{\partial C_A}{\partial\vec{x}} + C_A k_j\,\frac{\partial b_j(\vec{x})}{\partial\vec{x}} + k_j\,\frac{\partial V_j(\vec{x})}{\partial\vec{x}} \tag{2}$$

A simplification results if the wave vector is sufficiently parallel to the magnetic field and the bulk velocity gradients are small compared to Alfvén speed gradients. For this case $|k_j \partial b_j(\vec{x})/\partial\vec{x}| \ll |$ and the first term in equation (2) dominates so that gradients in the ambient Alfvén speed control the change in the wave vector. These conclusions are empirically verifiable as we shall see later.

## EXPERIMENT DESCRIPTION

The Pioneer 6 spacecraft was launched on 16 Dec. 1965 into a heliocentric orbit and within a day the probe was well outside magnetospheric influence in interplanetary space. The Ames plasma probe [Wolfe and McKibben, 1968; Smith and Day, 1971] sampled the flux and energy per change as a function of direction. Full energy/angular scans were made each 400 spacecraft

revolutions so that plasma parameters are computed (on the basis of an isotropic temperature) every 412 sec. This defines the high frequency cutoff of the plasma data used. The only plasma parameter crucial to the analysis is the proton density which enters the Alfvén speed as $N_p^{-1/2}$ Therefore, typical errors in $N_p$ of $10 - 15\%$ are not crucial.

The magnetic field experiment [described by *Scearce et al.*, 1968] was a monoaxial fluxgate magnetometer which sampled a total vector field in one second. The analog to digital conversion introduces an error of $\pm 0.25$ gamma while the spacecraft field at the sensor location was estimated at less than 0.3 gamma. Averages of this data over 30-sec intervals are used in the analysis of this paper. Most data used was taken when the bit rate was 512 bits/sec. The coordinate frame is the right-handed solar ecliptic system in which the X axis points from the spacecraft (inward) to the sun and the Z axis to the north ecliptic pole (Figure 1).

## DETERMINATION OF THE WAVE NORMAL DIRECTION

The real symmetric matrix $T_{ij} = \langle B_i B_j \rangle - \langle B_i \rangle \langle B_j \rangle$ formed from components (i,j = 1,2,3) of any vector field in an inertial coordinate frame will have eigen values $\lambda_3 \geq \lambda_2 \geq \lambda_1$ and corresponding eigen vectors $\hat{M}_3$, $\hat{M}_2$, and $\hat{M}_1$ which define the principal axes of a 'variance' ellipsoid. $\hat{M}_3$ is the direction of maximum variation, $\hat{M}_1$ the direction of minimum variation, and $\hat{M}_2$ completes the orthogonal set. If $\lambda_1 = \lambda_2 = \lambda_3$ the ellipsoid is a sphere and the variance of the vector field is isotropic, whereas if $\lambda_1/\lambda_2 \ll 1$ the variance is strongly oriented in a plane whose normal is $\hat{M}_1$ (the direction of minimum variance).

A variance matrix analysis is used on the 30 sec averages of the Pioneer 6 magnetometer data as a basis for determining the direction of the wave propagation $\hat{k}$. If the magnetic fluctuations result from the propagation of a large amplitude Alfvén wave (or an ensemble of waves propagating in the same direction) the matrix $T_{ij}$ will have a well defined direction of minimum variance parallel (or antiparallel) to the wave vector(s). (In the small amplitude limit $\lambda_1/\lambda_2 = 1$ and the plane is undefined.)

The ambient mesoscale magnetic field, through which the microscale Alfvén waves propagate, is often very inhomogeneous (see, e.g., *Brandt*, 1970). Such large-scale gradients may effect the eigen vectors $\hat{M}$. Suppose, for example, the wave normal is constant while the ambient magnetic field changes direction on a scale $L \gg k^{-1}$. Then for a given $\measuredangle$ $(\hat{k},\hat{b})$ the magnetic vector moves as constrained by the homogeneous case in a plane whose normal is parallel (or antiparallel) to $\hat{k}$. But the variance matrix on $B_i$ contains, besides power from the Alfvénic fluctuations (which by themselves have a minimum variance along $\overleftarrow{k}$), power from the large-scale change in the direction of $\overleftarrow{B}$ (which by itself has a minimum variance nonparallel to $\hat{k}$). Therefore, the background field can contribute to the variance matrix and change the direction of minimum variance from along $\hat{k}$. To suppress the contribution to $T_{ij}$ of a slowly varying background field we will use a matrix based on a suitably defined 'local average' (or smoothed) magnetic vector. We define

$$T_{ij} = \langle \Delta B_i \Delta B_j \rangle - \langle \Delta B_i \rangle \langle \Delta B_j \rangle$$

where

$$\Delta B_i = B_i - B_i^S ; \quad \text{note } \langle \Delta B_i \rangle \neq 0$$

$B_i$ = i component of the magnetic field

$B_i^S$ = i component of the digitally smoothed set of $B_i$

to determine the minimum variance direction of the magnetic vector. (This is in contrast to *Belcher and Davis*, 1971, who used the components $B_i$ to form the variance matrix.) (For example, consider a constant vector $\overleftarrow{A}$ upon which is superimposed a vector $\overleftarrow{a}$ varying randomly parallel to any fixed plane. The matrix $T_{ij}$ contains power only from $\overleftarrow{a}$ and gives the minimum variance direction $\hat{M}_1$ normal to the plane. Now let $\overleftarrow{A}$ remain constant in magnitude but, confined to another plane not parallel to the first, slowly vary in direction. Subtraction of the smoothed $\overleftarrow{A} + \overleftarrow{a}$ vector from $\overleftarrow{A} + \overleftarrow{a}$ will suppress contributions to $T_{ij}$ from changes in $\overleftarrow{A}$, and $\hat{M}_1$ will remain normal to $\overleftarrow{a}$.) The smoothing is performed on each hour of 30-sec magnetic field averages with a 225-sec half-width Bartlett lag window [see *Jenkins and Watts*, 1969]. This

procedure narrows the effective bandwidth entering the variance matrix to between 0.03 Hz and about 0.003 Hz, thereby limiting the range of wavelengths accepted by $T_{ij}$ and reducing the total power contribution to the matrix. Wave normals from this band will be compared to plasma gradients computed from 900 sec averages; therefore, the smallest inhomogeneity will be approximately 3-30 times larger than a typical wavelength. This frequency band accepted by $T_{ij}$ is just above the high frequency cutoff of the plasma data used by Belcher and Davis [1971] to find the necessary velocity and magnetic correlations and establish the presence of Alfvén waves in the solar wind. Thus, strictly speaking, it cannot be proved that the magnetic fluctuations above 0.003 Hz are Alfvén waves. However, other hydromagnetic wave modes are expected to undergo severe damping [Barnes, 1966]. Also, interplanetary fluctuations have been shown to dominate the microstructure at least 50% of the time over a broad frequency range up to 0.003 Hz [Belcher and Davis, 1971] and there is no evidence to make us expect different microstructure at somewhat higher frequencies. As will be discussed in greater detail in the next section, the magnetic vector in this frequency range often behaves consistently with Alfvén propagation. Specifically, about 56% of the time studied, the largest eigen value of $T_{ij}$ is at least six times as large as the variance of the field magnitude. These observations would be expected from a large amplitude Alfvén wave. Convected static structure would not generally yield fluctuations in B consistent with these results.

We have selected 900-sec blocks of magnetic data if they meet two criteria: (1) The matrix eigen values are required to be $\lambda_3/\lambda_2 \geq 1.8$, $\lambda_2/\lambda_1 \geq 2.0$ to insure the existence of a reasonably well-defined direction of minimum and maximum variance. While somewhat arbitrary, the criterion on $\lambda_3/\lambda_2$ would be met by a large amplitude Alfvén wave if the magnetic vector fluctuated less than about 70° from the background field (this can be seen from simple geometrical considerations using Figure 1). The criterion on eigen value ratios would be met by a set of 30 vectors from a random parent distribution about 5% of the time [see Siscoe and Suey, 1972]; (2) The largest eigen value of the variance matrix had to be at least six times the variance of the field magnitude. This method was used as a simple means of identifying intervals high in Alfvénic content and discriminating against non-Alfvénic and static structure such as tangential discontinuities. If both of these tests were

not passed, the data block was rejected. All other blocks with no data gaps were used in the analysis. This magnetometer data was taken from 0900 UT 26 Jan. through 1700 UT 9 Feb. 1966 and included the passage of two high velocity (with mean velocities of about 550 and 500 km/sec) and two low velocity streams (mean velocities each about 350 km/sec).

The eigen vector $\hat{M}_1$ which is associated with the smallest eigen value $\lambda_1 \ll \lambda_2$ is normal to the plane in which the tip of the magnetic vector tends to move (an Alfvén wave, for example). The wave vector $\overline{k}$ is also normal to this plane but may be parallel or antiparallel to $\hat{M}_1$. Unless otherwise stated, it is assumed that $\hat{M}_1$ points out from the sun ($\hat{M}_1 \cdot \hat{X} < 0$), since *Belcher and Davis* [1971] found velocity and magnetic fluctuations consistent only with outward propagation.

## RESULTS AND DISCUSSION

Between 26 Jan. and 9 Feb. 1966, $T_{ij}$ was calculated for 832 900-sec blocks of 30-sec-average Pioneer 6 magnetometer data. (The integrated power from 900 sec of microscale fluctuations is ample to define a statistically significant variance matrix.) Of these intervals 307 met the screening criteria described above. About 29% of the 832 blocks were eliminated by constraint (1) and 44% by constraint (2) as defined in the previous section. A time series plot of the solar ecliptic latitude and longitude of the mean field for each 900-sec block (solid line) is shown in Figure 2 for a high velocity stream (mean velocity about 550 km/sec), its trailing edge, and part of the following low velocity stream (about 350 km/sec). The corresponding directions of $\hat{M}_1$ are given by the unconnected points with the $\not\triangleleft(\hat{M}_1,b)$ and $\not\triangleleft(\hat{M}_1,X)$ shown below. ($\hat{X}$ is the solar direction.) The vertical lines mark data gaps.

It is fairly clear that, while there are many isolated exceptions, $\hat{M}_1$ tends to be parallel or antiparallel to the mean magnetic vector. The distribution of $\hat{M}_1$ in eight equal solid angle increments about $\hat{b}$ is given in Figure 3. The $\not\triangleleft(\hat{M}_1,b)$ is defined here by the acute angle between coplanar lines parallel to $\hat{M}_1$ and $\hat{b}$. Also shown are the distributions of the minimum variance and mean magnetic field directions in equal solid angle increments about the antisolar direction. ($\hat{M}_1$ points out from the sun. Comparison of the two distributions is easier if the mean field is

also directed out. Therefore, when $\hat{b} \cdot \hat{X} > 0$ the field vector is reflected through the origin and the angle calculated with the antisolar direction.) These distributions do not change significantly when criterion (2) is changed to $\lambda_3/\sigma^2 |B| \geq 10$, thereby constraining the field magnitude to be even more consistent with Alfvén propagation. It is clear that the direction of minimum variance is preferentially oriented along B. About 87% of the time $\angle(\hat{M}_2,\hat{b})$ is less than $41°$. The corresponding result of *Belcher and Davis* [1971] was 77%. A direct comparison is difficult because of the narrower bandwidth, different variance matrix and the screening procedure used in obtaining the former result. It is significant that there are no other peaks in the $\angle(\hat{M}_1,\hat{b})$ or $\angle(\hat{M}_1,\hat{X})$ distributions. If other magnetic microstructure (either propagating or static) in the frequency range from 1/30 sec to 1/300 sec have planes of minimum variance of another preferred orientation to $\hat{b}$ or $\hat{X}$ (1) their total power contribution is completely masked by the (assumed) Alfvén component or (2) they were in some way eliminated by the screening criteria described above.

The effects (or lack of them) on $\hat{M}_1$ from changes in $\hat{b}$ can be seen in Figure 4. It is clear that $\angle(\hat{M}_1,\hat{b})$ has about the same distribution when the background field rapidly changes direction and when it is quiet. There seems to be no correlation between the two variables in either high velocity streams (where the correlation between magnetic and velocity fluctuations suggests that Alfvén microstructure dominates) or the low velocity streams (where the Alfvén microstructure is less). Table 1 confirms that there is essentially the same $\angle(\hat{M}_1, \hat{b})$ distribution in both cases.

Let us further examine the relation between $\Delta\hat{b}$ and $\angle(\hat{M}_1,\hat{b})$. (We define $\Delta\hat{b} = \hat{b}(t) - \hat{b}(t + \Delta t)$ and compare this with $\angle[\hat{M}_1(t + \Delta t), \hat{b}(t + \Delta t)]$ assuming outward propagation over the $\Delta t = 900$-sec interval.) Consider the plane defined by the vectors $\hat{b}$ and $\hat{M}_1$. In Figure 5 the orientation of this plane is represented by a chord between the intersection of the two vectors on the unit sphere. The positions of $\hat{b}$ are numbered consecutively, the location of the number marking the interaction of $\hat{b}$ on the sphere—the opposite end of the chord locates $\hat{M}_1$. When the chord is missing the direction of minimum variance is not well-defined and was eliminated by the data screening. The example is fairly typical and represents a magnetically active period in a low velocity stream. In this interval $\hat{b}$ moved onto the inward hemisphere (positions 26 and 27) and the chords for these are not shown. Note that there is no preferred orientation of $\hat{M}_1$ relative to the movement of $\hat{b}$.

For a more quantitative understanding of the $(\hat{M}_1,\hat{b})$ plane orientation let us define

$\tan \beta = \Delta\theta/\Delta\phi$ where $\Delta\theta$ is the longitude difference between a pair of $\hat{M}_1$, $\hat{b}$ and $\Delta\phi$ is the latitude difference (if $\hat{b}\cdot\hat{X} > 0$, $\hat{b}$ is reflected through the origin and the new position angles are used). The distribution of $\beta$ is shown in Figure 6. There may be a slight north-south preference, but the trend is weak and may well be attributed to statistical fluctuations.

The analysis reported to this point indicates little or no relation between the direction of the Alfvén wave vector relative to $\hat{b}$ and inhomogeneities of the ambient magnetic field direction. There are principally three reasons for this conclusion: (1) $\hat{M}_1$ is not constant or random in the space craft frame, but tends to follow the mean field direction; (2) The distribution of $\angle(\hat{M}_1,\hat{b})$ is not noticeably different when $\Delta\hat{b}$ is large or small—there is no correlation between $\Delta\hat{b}$ and $\angle(\hat{M}_1,\hat{b})$; (3) There seems to be no orientation of $\hat{M}_1$ to $\hat{b}$ statistically correlated with $\Delta\hat{b}$. Two conclusions can now be drawn. First, the data is consistent with large amplitude Alfvén wave propagating, by and large, along the ambient magnetic field. Secondly, deviations of the wave vector from this orientation are not caused by directional changes in the ambient field.

If the unperturbed state is one in which $\hat{k}$ is parallel (or antiparallel) to the ambient field, we might inquire about plausible explanations for deviations of $\hat{M}_1$ from $\hat{b}$. It is possible (but not likely) that some of the magnetic fluctuations are not Alfvénic but result from one or more other MHD wave modes or that they are static—e.g., tangential discontinuities. Especially during magnetically quiet interplanetary conditions, constant or changing space craft fields could bias $\hat{M}_1$ and $\hat{b}$ by small amounts. Of course, any combination of these sources (along with others) may contribute to $\angle(\hat{M}_1,\hat{b})$, in which case their identification would be difficult.

On the other hand, $\angle(\hat{M}_1,\hat{b})$ may be related to properties of the ambient plasma. In the light of equation (2) we might expect inhomogeneities in the local Alfvén speed and wind bulk velocity to scatter the wave vector. To test this hypothesis let us propose three simplifying postulates: (1) The wave vector is parallel or antiparallel to the ambient magnetic field except (2) as perturbed by local gradients in the Alfvén speed, $C_A$. (3) The directional change in $\hat{k}$ is proportional to $|\nabla C_A|$.

A reasonably reliable test of the hypothesis is possible using the Pioneer 6 plasma and magnetic data. Gradients in $\overleftarrow{V}(x)$ and $C_A(\overleftarrow{x})$ are probably about the same magnitude. It will be demonstrated that statistically significant regions can be found where the expected relationship exists between the wave normal and Alfvén speed gradients (neglecting complications due to velocity gradients although we have not shown that they can always be neglected). We will, therefore, examine only the qualitative relationships between the Alfvén speed and $\hat{M}_1$. Temporal changes in the direction of the wave vector will be measured by $\measuredangle(\hat{M}_1,\hat{b})$. Gradients in the Alfvén speed will be approximated by changes in $C_A$, $|\Delta C_A|$, between the appropriate $\Delta t = 900$-sec intervals assuming wave propagation away from the sun. Of course, for a time independent $C_A$ in the plasma rest frame we have $|\Delta C_A| = |\overleftarrow{V}\cdot\nabla C_A|\Delta t$ so that $|\Delta C_A|/V\Delta t$ is a measure of the lower bound on $|\nabla C_A|$. A linear correlation between $\measuredangle(\hat{M}_1,\hat{b})$ and $|\nabla C_A|$ could be demonstrated by a plot of $|\nabla C_A|$ as a function of $\measuredangle(\hat{M}_1,\hat{b})$–the result being points near some straight line. The same correlation would show up with $|\Delta C_A|$ replacing $|\nabla C_A|$(implying a gradient over $V\Delta t$) but some of the points would be moved down (to lower $|\Delta C_A|$) when $|\Delta C_A|/V\Delta t < |\nabla C_A|$, resulting in a spreading of the points between the line of correlation $(\overleftarrow{V}\|\nabla C_A)$ and $|\Delta C_A| = 0\,(\overleftarrow{V}\bot\nabla C_A)$.

In an attempt to further isolate the regions of best Alfvén activity the data from high and low velocity streams were kept separate and both are shown in Figure 7. Neither case shows linear correlation between the variables. For example, the correlation for the high velocity streams (crosses) is about 0.05. A least squares straight line for this same data has a slope of $0.24\pm0.39\times10^6$ cm/deg sec and intercept of $0.41\times10^6$ cm/sec. It is apparent, however, that the high velocity stream data and, to a lesser extent, those from the low velocity streams (including the leading edge or interaction region) have the qualitative features consistent with our hypothesis based on equation (2). That is, a hypothetical line of correlation can be constructed which lies above most of the data points. We may, therefore, conclude that gradients of the ambient Alfvén speed satisfying the geometrical approximation may be one mechanism for the scattering of the Alfvén wave normal from the direction of the local interplanetary magnetic field.

## ROLE OF DISCONTINUITIES

As pointed out in the introduction, both propagating and nonpropagating discontinuities are seen in the interplanetary plasma. These are usually defined as transients with characteristic times in the spacecraft frame of less than $\sim 1$ min (e.g. Burlaga 1969, 1971). In reality there is no natural break between transient and continuous fluctuations — the distinction is always somewhat arbitrary. No attempt has been made in this analysis to delete the more discontinuous events but some conclusions can be made about statistical properties of discontinuities from results already reported.

Any microstructure with sufficient power in the bandwidth accepted by the variance matrix will produce a "peak" in the $\measuredangle(\hat{M}_1,\hat{b})$ distribution (Figure 3), if it has a plane of minimum variance of some preferred orientation to the mean magnetic field. For example, the tangential pressure balance would ideally yield $\measuredangle(\hat{M}_1,\hat{b}) = 90°$. Of course, in general, this structure involves a change in the length of the magnetic vector and would therefore be screened from the data. As noted earlier, no significant maximum appears at $90°$ in Figure 3 (see Table 1 also). There is a maximum at $90°$ in the corresponding distribution of *Belcher and Davis* [1971]. They made no attempts in their analysis to eliminate data blocks which contained excessive non-Alfvénic structure. It is therefore reasonable to attribute this peak to the presence of tangential discontinuities.

The rotational discontinuity is only a sharply crested Alfvén wave and therefore a subclass of all Alfvénic fluctuations. However, *Turner and Siscoe* [1971] have pointed out that the discontinuous type of Alfvénic fluctuation has a polarization plane (defined by $\overleftarrow{B}_{initial} \times \overleftarrow{B}_{final}$) with a persistent southward component (about $30°$ south latitude). The normal for the corresponding plane of the more continuous Alfvénic fluctuations is [*Belcher and Davis*, 1971] essentially in the ecliptic plane. The subset of rotational discontinuities are unique in this respect from the parent group. Their wave normal could also be preferentially aligned differently relative to the background field. If so, and if their power contribution during the time studied is comparable to that of the background noise, a peak will appear in the $\measuredangle(\hat{M}_1,\hat{b})$ distribution. It appears from Figure 3 that the discontinuous Alfvénic fluctuations also propagate close to the ambient magnetic field direction (assuming statistically significant power contribution) and are not different in this respect from Alfvén waves.

## SUMMARY AND CONCLUSIONS

It has been shown that about 60% of the time during the 15 days studied, the microscale magnetic vector (0.03 Hz to about 0.003 Hz) moves as would be consistent with propagating Alfvén waves. This result is in general agreement with the findings of *Belcher et al.* [1969] and *Belcher and Davis* [1971] for the frequency range just below this. In addition, the phase velocities of these Alfvén waves are evidently strongly oriented along the ambient magnetic field. As *Belcher and Davis* [1971] point out, if the Alfvén wave sources are all within the Alfvénic critical point from the sun, only those propagating out from the sun will reach the super-Alfvénic solar wind. This, however, does not explain the close relation between $\hat{k}$ and $\hat{b}$. This preferential orientation of $\hat{k}$ has not been predicted. As a matter of fact, *Barnes* [1969] predicts that Alfvén wave normals will be geometrically refracted by the solar wind expansion such that at 1 AU they will be essentially radial. His arguments are based on a wave source inside the Alfvénic point producing waves which are convected through a strictly spiral magnetic field with no *local* (mesoscale or microscale) inhomogeneities. We know, in fact, that very seldom is such an ideal situation realized. Rather, abundant coronal irregularities (streamers, for example) imply significant inhomogeneities near the source, and interplanetary probe measurements imply the same for regions near 1 AU. This local structure may well determine wave properties in the several wavelengths which these waves propagate during their convection to 1 AU. In this context, it is difficult to conceive preferential refraction of wave normals to directions along the magnetic field lines. A possible alternative, however, may be selective damping of randomly refracted waves. *Belcher and Davis* [1971] advance an explanation for the power anisotropy of the solar wind magnetic fluctuations based on the coupling of the Alfvén mode to the magnetosonic modes. An extension of this mechanism may explain the orientation of $\overleftarrow{k}$ along the field lines. If, by increasing $\measuredangle(\overleftarrow{k},B)$, Alfvén waves couple with the strongly damped magnetosonic modes, or if they become subject to damping from microscale irregularities violating the geometrical approximation [*Valley*, 1971], it is likely that at 1 AU the surviving waves will be those strongly aligned with the magnetic field.

It should be pointed out that what we have defined in this paper as the ambient magnetic field (scale lengths $\gtrsim$ V X 900 sec) is also largely Alfvénic [*Belcher and Davis*, 1971] and

therefore propagating. It is not clear what consequences this has on the conclusions reached about the orientation of wave normals along the background field.

Assuming a preferential orientation of $\hat{k}$ along $\hat{B}$, deviations of $\hat{k}$ from the background field are more easily explained. Directional changes in the background magnetic field are shown to have no perceptible correlation with $\measuredangle(\hat{k},\hat{B})$, whereas inhomogeneities in the ambient Alfvén speed are a likely source for the scattering of $\hat{k}$ from $\hat{B}$. This is theoretically expected if the preferred state is one in which the wave normal lies along the ambient field.

The role of discontinuities in the analysis is less certain since no individual events were identified. It is safe, however, to conclude that if the integrated power of rotational discontinuities is comparable to that of the more continuous Alfvén fluctuations over the time studied, both propagate very nearly along the magnetic field lines.

REFERENCES

Barnes, A., Collisionless damping of hydromagnetic waves, *Phys. Fluids, 9,* 1483, 1966.

Barnes, A., Collisionless heating of the solar wind plasma II. Application of the theory of plasma heating by hydromagnetic waves, *Astrophys. J., 155,* 311, 1969.

Barnes, A., Theoretical constraints on the microscale fluctuations in the interplanetary medium, *J. Geophys. Res.*, *76*, 7522, 1971.

Belcher, J. W., L. Davis, and E. J. Smith, Large-amplitude Alfvén waves in the interplanetary medium: Mariner 5, *J. Geophys. Res.*, *74*, 2302, 1969.

Belcher, J. W., and L. Davis, Large-amplitude Alfvén waves in the interplanetary medium, 2, *J. Geophys. Res.*, *76*, 3534, 1971.

Brandt, John C., *Introduction to the solar wind*, 197 pp., W. H. Freeman and Company, San Francisco, Calif., 1970.

Burlaga, L. F., Micro-scale structures in the interplanetary medium, *Solar Phys.*, *4*, 67, 1968.

Burlaga, L. F., Directional discontinuities in the interplanetary magnetic field, *Solar Phys.*, *7*, 54, 1969.

Burlaga, L. F., Nature and origin of directional discontinuities in the solar wind, *J. Geophys. Res.*, *76*, 4360, 1971.

Colburn, D. S., and C. P. Sonett, Discontinuities in the solar wind, *Space Sci. Rev.*, *5*, 439, 1966.

Coleman, P. J., Variations in the interplanetary magnetic field: Mariner 2, *J. Geophys. Res.*, *71*, 5509, 1966.

Coleman, Paul J., Wave-like phenomena in the interplanetary plasma: Mariner 2, *Planetary Space Sci.*, *15*, 953, 1967.

Jenkins, G. M., and D. G. Watts, *Spectral Analysis and its Applications*, 525 pp., Holden-Day, San Francisco, Calif., 1969.

Kantrowitz, A., and H. E. Petschek, *Plasma Physics in Theory and Application*, edited by W. B. Kunkel, McGraw-Hill, New York, 1966.

Scearce, C. S., C. Ehrmann, S. C. Cantrorano, and N. F. Ness, Magnetic field experiment: Pioneers 6, 7, and 8, *NASA—Goddard Space Flight Center preprint* X-616-68-370.

Siscoe, G. L., and R. W. Suey, Significance criteria for variance matrix applications, *J. Geophys. Res.*, *77*, 1321, 1972.

Smith, Z. K., and J. R. Day, A mathematical model of the arc Pioneer 6/7 plasma probe, *Rev. Sci. Instr.*, *42*, 968, 1971.

Turner, J., and G. L. Siscoe, Orientation of rotational and tangential discontinuities in the solar wind, *J. Geophys. Res.*, *76*, 1816, 1971.

Unti, T. W. J. , and M. Neugebauer, Alfvén waves in the solar wind, *Phys. Fluids*, *11*, 563, 1968.

Valley, G. C., Propagation of hydromagnetic waves in a stochastic magnetic field, *Astrophys J.*, *168*, 251, 1971.

Weinberg, S., Eikonal method in magnetohydrodynamics, *Phys. Rev.*, *126*, 1899, 1962.

Wolfe, J. H., and D. D. McKibbin, Pioneer 6 observations of a steady-state magnetosheath, *Planetary Space Sci.*, *16*, 953, 1968.

TABLE 1. Distribution of $\sphericalangle(\hat{M}_1,\hat{b})$ in Equal Solid Angle Increments

For High and Low Velocity Streams

(taken from same data as Figure 4)

| | 0/29 | 29/41 | 41/51 | 51/60 | 60/68 | 68/76 | 76/83 | 83/90 | 90/97 | 97/104 | 104/112 | 112/120 | 120/129 | 129/139 | 139/151 | 151/180 |
|---|---|---|---|---|---|---|---|---|---|---|---|---|---|---|---|---|
| High Velocity Streams % | 74.4 | 8.5 | 2.4 | 3.6 | 1.2 | 1.2 | 3.6 | 1.2 | 1.2 | 0 | 1.2 | 1.2 | 0 | 0 | 0 | 0 |
| Low Velocity Streams, % | 75.2 | 9.1 | 2.4 | 1.8 | 0.6 | 2.4 | 1.2 | 0 | 0.6 | 0.6 | 0 | 0.6 | 0.6 | 0 | 0.6 | 3.0 |

## FIGURE CAPTIONS

Fig. 1. The solar ecliptic coordinate system and the relevant geometry for a large amplitude Alfvén fluctuation $\Delta \vec{B}_\perp$ ($\Delta \vec{B}_\perp \cdot \vec{k} = 0$).

Fig. 2. Time series display for the latitude ($\theta$) and longitude ($\phi$) of the ambient magnetic field (line) and the direction of the minimum variance with $\hat{M}_1 \cdot \hat{X} < 0$ (points). Each point represents a 900-sec interval; missing points indicate an interval eliminated by the screening procedure described in the text. The angles between $\hat{M}_1$ and the mean field ($\angle(\hat{M}_1,\hat{b})$) and $\hat{M}_1$ and the solar direction ($\angle(\hat{M}_1, -\hat{R})$) are also shown. Vertical lines mark data gaps.

Fig. 3. Distributions of $\angle(\hat{M}_1,\hat{b})$ and $\angle(\hat{b},\hat{R})$ (both defined as acute angles) and $\angle(\hat{M}_1,\hat{R})$ are shown for eight equal solid angle increments. Each angle is defined in the text.

Fig. 4. $\angle(\hat{M}_1,\hat{b})$ is shown relative to changes in the mean field direction in high velocity streams and their trailing edges (crosses; 0900 UT 26 Jan. 66 to 0200 UT 28 Jan. 66 and 1300 UT 4 Feb. 66 to 0200 UT 7 Feb. 66) and in a low velocity stream and on the leading edge of a high velocity stream (points; 0100 UT 29 Jan. 66 to 1300 UT 4 Feb. 66).

Fig. 5. Orientation of the $(\hat{M}_1,\hat{b})$ plane shown by a chord between $\hat{b}$ (numbered consecutively on the unit sphere) and $\hat{M}_1$. Data is from a low velocity stream between 0300 and 1100 UT 29 Jan. 66.

Fig. 6. The orientation of $\hat{M}_1$ relative to $\hat{b}$ on the unit sphere is defined by $\tan \beta$ = (latitude difference/longitude difference). The number of cases of $\beta$ in each $60°$ increment is shown. The mean and one standard deviation are indicated assuming the parent distribution is Poisson.

Fig. 7. $\angle(\hat{M}_1,\hat{b})$ vs. $|\Delta C_A|$ for two high velocity streams and their trailing edges (crosses; 0900 UT 26 Jan. 66 to 0200 UT 28 Jan. 66 and 1300 UT 4 Feb. 66 to 0200 UT 7 Feb. 66) and for two low velocity streams and the leading ege of a high velocity stream (points; 0100 UT 29 Jan. 66 to 1100 UT 4 Feb. 66 and 0900 UT 7 Feb. 66 to 0500 UT 9 Feb. 66).
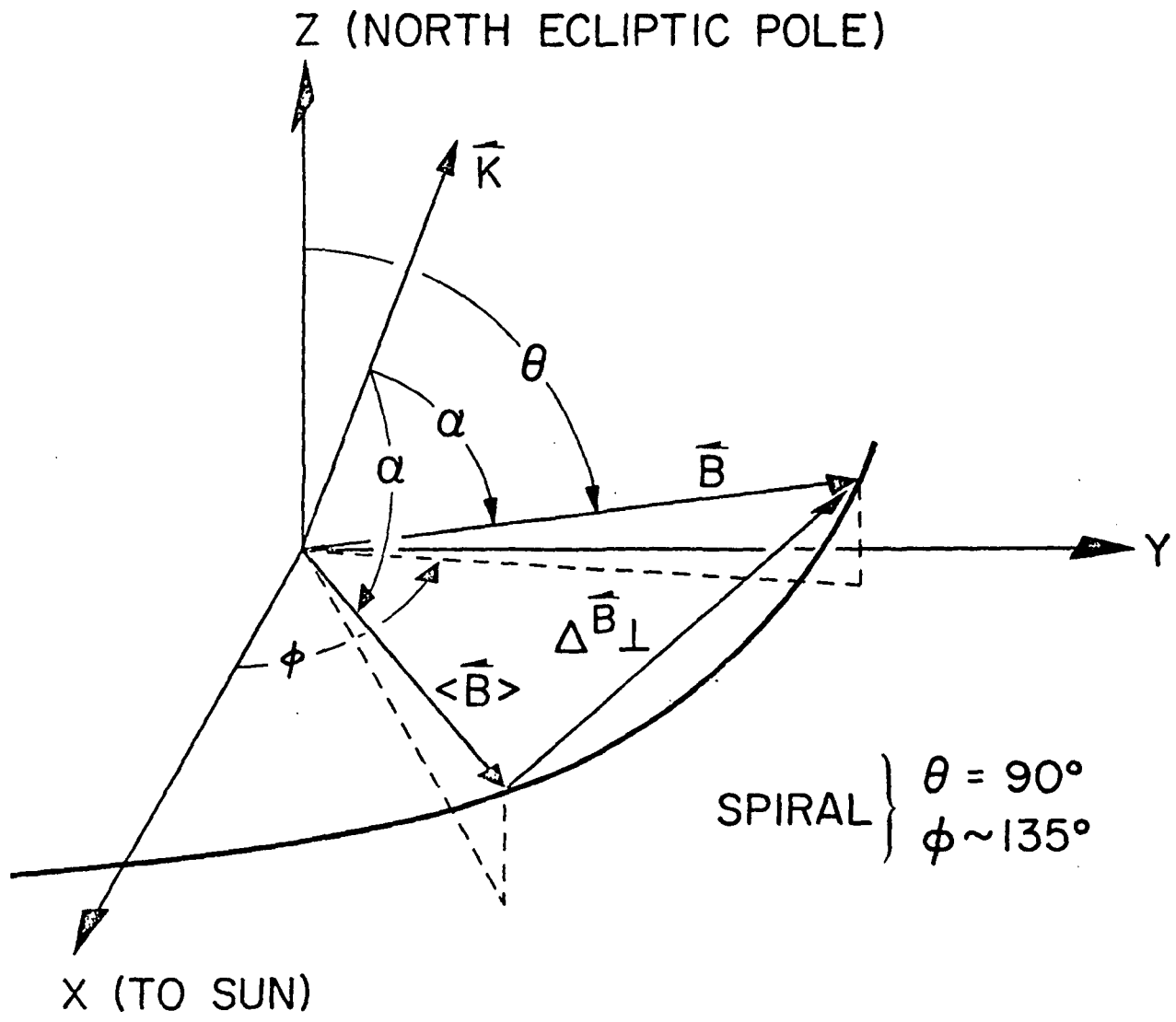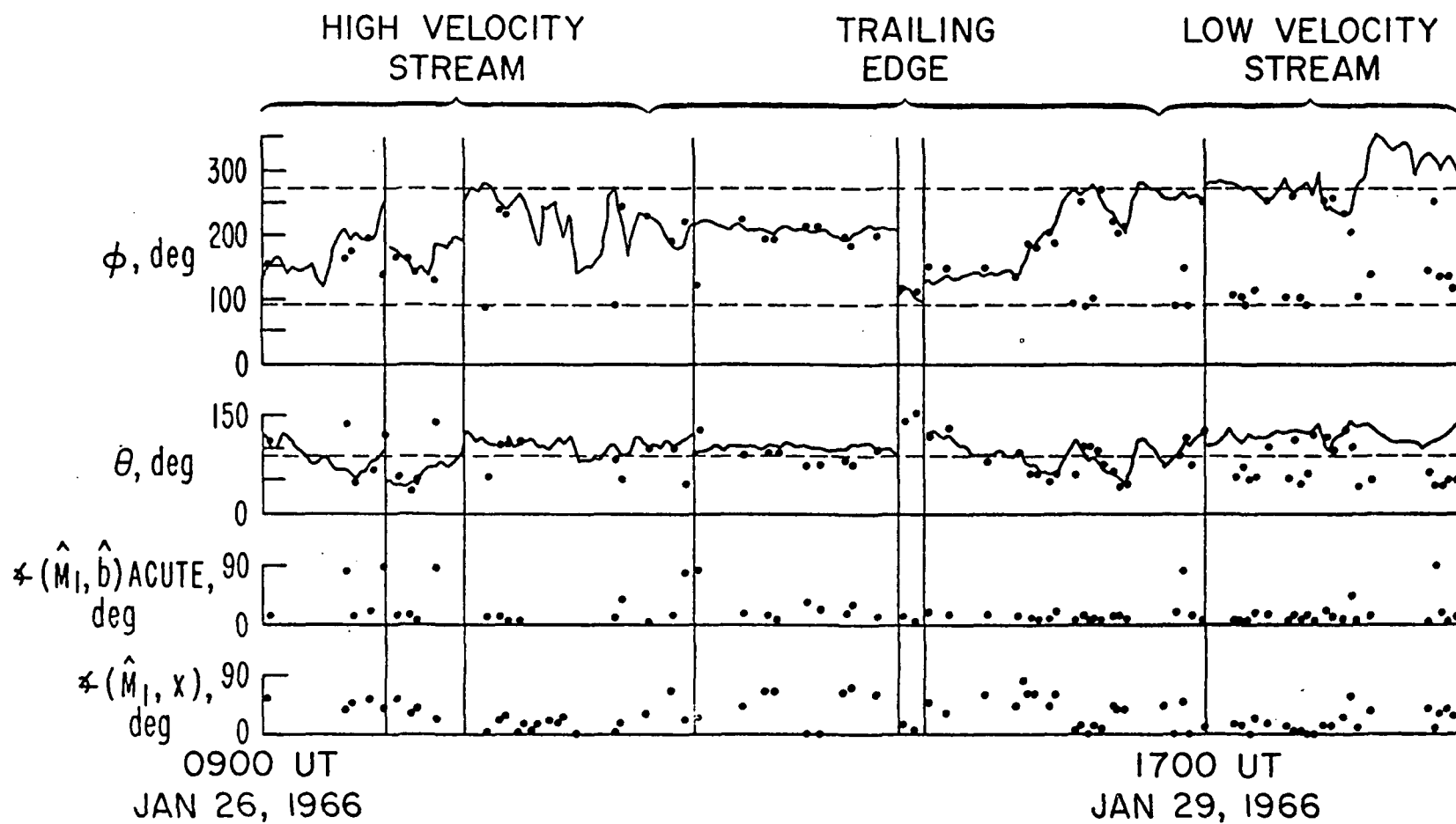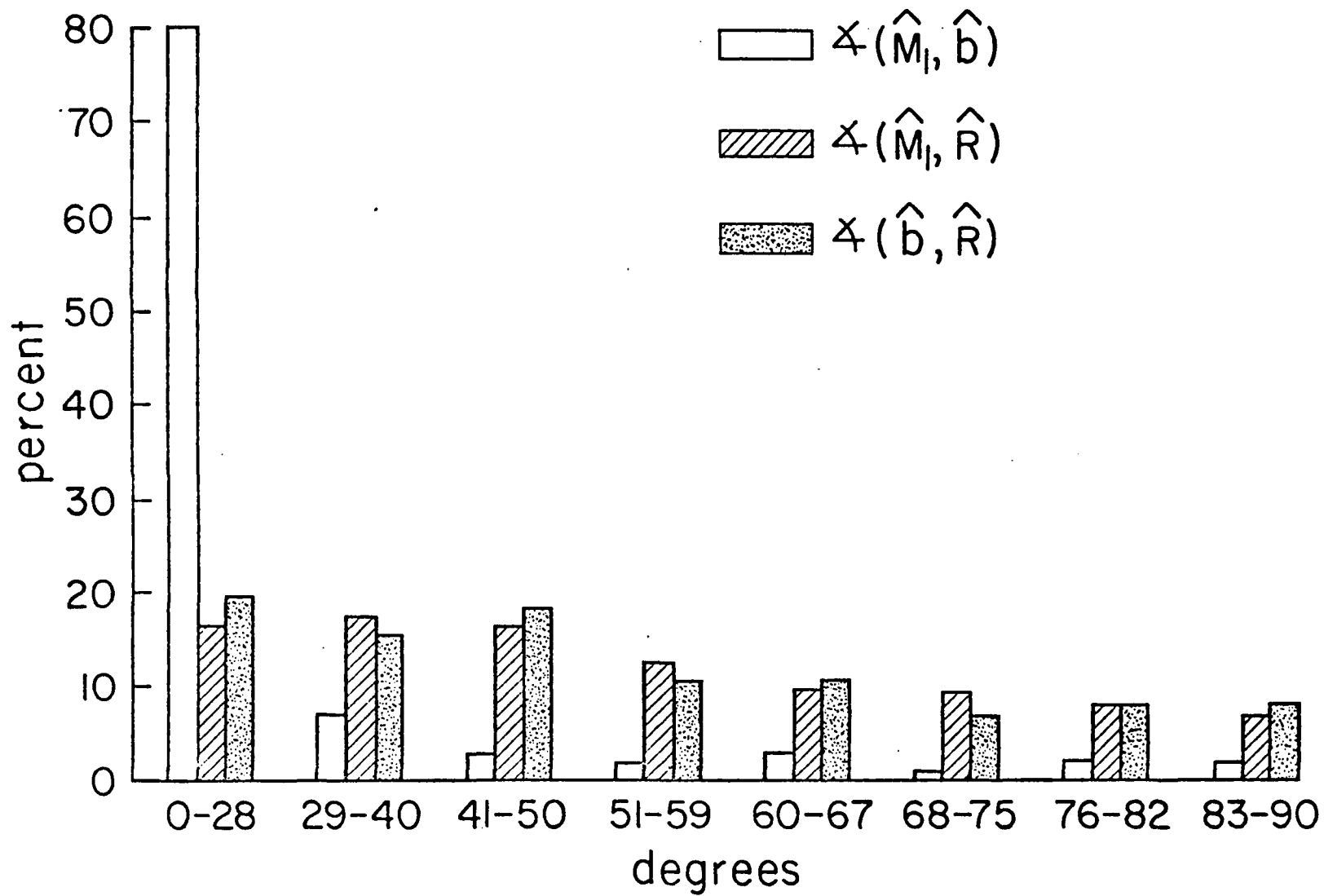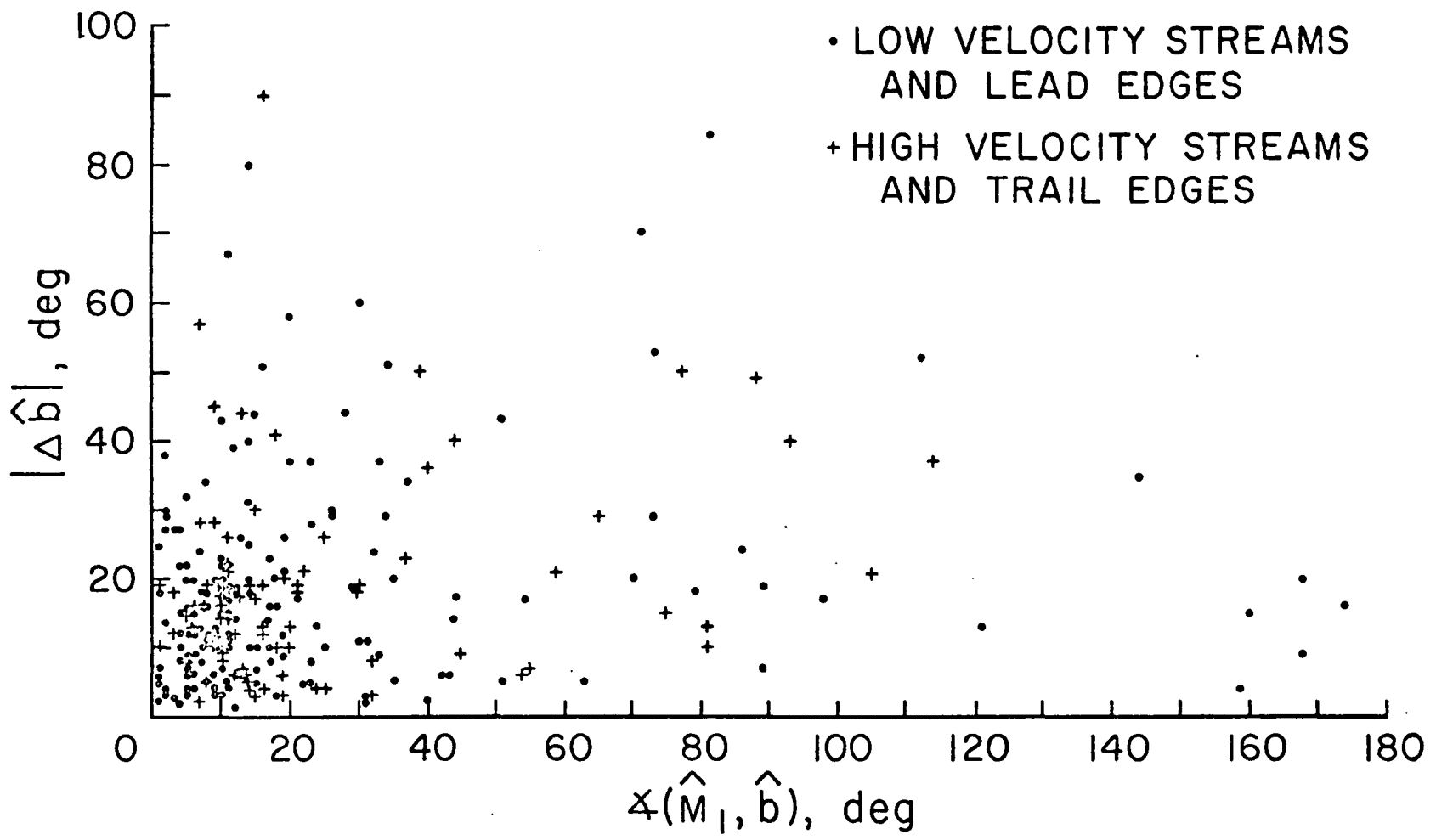
Fig. 1

Fig. 2

Fig. 3

Fig. 4

Fig. 5

0°

100

270° 90°

180°

Fig. 6

Fig. 7